

Mixed electroweak-QCD corrections to $e^+e^- \rightarrow HZ$ at Higgs factory

Qing-Feng Sun ^{*}, ^{1,2} Feng Feng [†], ^{3,2} Yu Jia [‡], ^{2,4,5} and Wen-Long Sang ^{§6}

¹*Department of Modern Physics, University of Science and Technology of China, Hefei, Anhui 230026, China*

²*Institute of High Energy Physics and Theoretical Physics Center for Science Facilities, Chinese Academy of Sciences, Beijing 100049, China*

³*China University of Mining and Technology, Beijing 100083, China*

⁴*School of Physics, University of Chinese Academy of Sciences, Beijing 100049, China*

⁵*Center for High Energy Physics, Peking University, Beijing 100871, China*

⁶*School of Physical Science and Technology, Southwest University, Chongqing 400700, China*

(Dated: October 11, 2018)

The prospective Higgs factories, exemplified by ILC, FCC-ee and CEPC, plan to conduct the precision Higgs measurements at the e^+e^- center-of-mass energy around 250 GeV. The cross sections for the dominant Higgs production channel, the Higgsstrahlung process, can be measured to a (sub-) percent accuracy. Merely incorporating the well-known next-to-leading order (NLO) electroweak corrections appears far from sufficient to match the unprecedented experimental precision. In this work, we make an important advancement toward this direction by investigating the mixed electroweak-QCD corrections to $e^+e^- \rightarrow HZ$ at next-to-next-to-leading order (NNLO) for both unpolarized and polarized Z boson. The corrections turn out to reach one percent level of the Born-order results, thereby must be incorporated in the future confrontation with the data.

PACS numbers: 12.15.Lk, 12.38.-t, 13.66.Fg, 14.80.Bn

Introduction. The ground-breaking discovery of the 125 GeV boson at CERN Large Hadron Collider (LHC) in 2012 has opened a new era in particle physics [1, 2]. It is of the highest priority to scrutinize the property of this Higgs-like boson, in order to penetrate into the mechanism of electroweak symmetry breaking, and to seek the footprint of new physics. In contrast to the enormous backgrounds at LHC, the clean environment renders the e^+e^- collider to be a much more appealing option to conduct precision Higgs measurements.

Recently, three next-generation e^+e^- colliders have been proposed to serve as Higgs factory: International Linear Collider (ILC) [3, 4], Future Circular Collider (FCC-ee) [5], and Circular Electron-Positron Collider (CEPC) [6, 7]. All of them intend to operate at center-of-mass (CM) energy within the $240 \sim 250$ GeV range, and plan to accumulate about $10^5 - 10^6$ Higgs boson events. Around such energy, the Higgsstrahlung process, $e^+e^- \rightarrow HZ$, becomes the dominant Higgs production channel, much more important than the WW/ZZ -fusion processes, and the recoil mass technique can be applied to precisely measure the HZ event yield and the Higgs boson mass. Consequently, $\sigma(e^+e^- \rightarrow HZ)$ is anticipated

to be measured to an exquisite accuracy, *e.g.*, 1.2% at ILC, 0.5% at CEPC, and 0.4% at FCC-ee. Moreover, various Higgs couplings, exemplified by $H \rightarrow gg, c\bar{c}$, can also be precisely measured at Higgs factory, otherwise very difficult to access at LHC. Furthermore, it has also been recently suggested that the $\sigma(HZ)$ could serve as a sensitive probe for various new physics scenarios [8–13].

Needless to say, in order to confidently interpret the future experimental measurements, one must develop a comprehensive knowledge on the Standard Model (SM) predictions to the Higgsstrahlung process. The leading order (LO) prediction to this process was known long ago [14–16]. The NLO electroweak corrections have also been available for a while, independently addressed by three groups [17–19]. For a light Higgs boson and at Higgs factory energies, the NLO weak corrections can reach a few percent level, thereby must be incorporated in phenomenological analysis.

To match the projected sub-percent accuracy of the cross section measurements at CEPC and FCC-ee, it seems compulsory to incorporate even higher order corrections. The next most important corrections are the $\mathcal{O}(\alpha^2)$ electroweak corrections and the mixed electroweak-QCD $\mathcal{O}(\alpha\alpha_s)$ corrections. While the former is exceedingly challenging to compute, the latter is much more tractable and may be more significant in magnitude owing to the occurrence of the QCD coupling constant. It is the very goal of this work to comprehensively investigate the $\mathcal{O}(\alpha\alpha_s)$ corrections to the Higgsstrahlung process at

^{*}qfsun@mail.ustc.edu.cn

[†]F.Feng@outlook.com

[‡]jiay@ihep.ac.cn

[§]wlsang@ihep.ac.cn

Higgs factory.

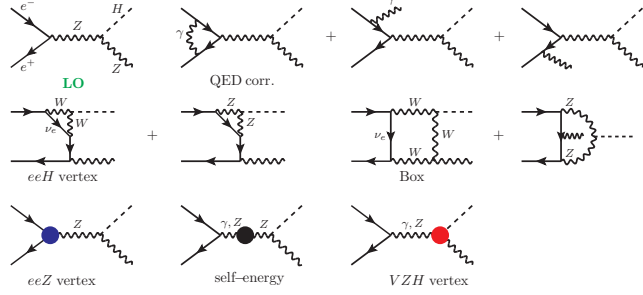


FIG. 1: LO diagram for $e^+e^- \rightarrow HZ$ and examples of QED $\mathcal{O}(\alpha)$ corrections and weak one-loop corrections, consisting of eeH vertex corrections, box diagrams, and corrections to the eeZ vertex, the γ/Z self-energy and VZH vertex. The latter three types of corrections also include $\mathcal{O}(\alpha\alpha_s)$ corrections as shown in Fig. 2.

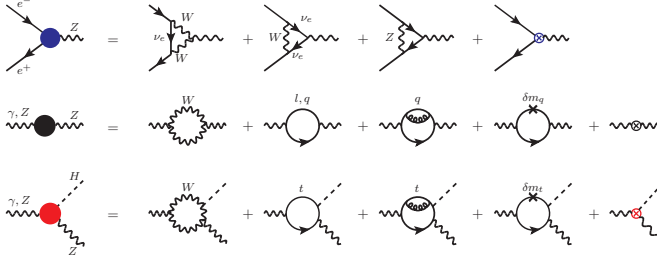


FIG. 2: Representative diagrams for the weak $\mathcal{O}(\alpha)$ and $\mathcal{O}(\alpha\alpha_s)$ corrections to the eeZ vertex, γ/Z self-energy, and VZH vertex. The cross represents the quark mass counterterm in QCD, a cap denotes the electroweak counterterm.

Leading-order results. By safely neglecting the electron mass owing to its exceedingly tiny Yukawa coupling, there is only a single s -channel Feynman diagram for the LO Higgsstrahlung process, as depicted in Fig. 1. In the CM frame, the amplitude for $e^+(k_1, -\sigma) + e^-(k_2, \sigma) \rightarrow H(p_H) + Z(p_Z, \lambda)$ reads:

$$\mathcal{M}_0^{\sigma, \lambda} = e^2 g_e^\sigma \frac{M_Z}{s w c_W} \frac{1}{s - M_Z^2} \bar{v}(k_1) \gamma^\mu \not{\epsilon}_\lambda^\sigma P_\sigma u(k_2), \quad (1)$$

where $P_\pm = \frac{1 \pm \gamma^5}{2}$ are chirality projectors, $\not{\epsilon}_\lambda^\mu$ denotes the polarization vector of the Z boson, with $\lambda = 0(\pm 1)$ being the longitudinal(transverse) polarization. $\sigma = \pm \frac{1}{2}$ represents the helicity of the incoming electron or positron (often we use the shorthand $\sigma = \pm$ for brevity). To warrant a nonvanishing amplitude, the positron must carry the opposite helicity with respect to the electron. We follow the conventions in [20] to define the Weinberg angle as $c_W \equiv \frac{M_W}{M_Z}$, and $s_W \equiv \sqrt{1 - c_W^2}$. The $Zf\bar{f}$ couplings g_f^\pm are defined following [19].

For simplicity, we will consider the unpolarized $e^+(e^-)$ beams, which is the case for CEPC and FCC-ee. The LO

differential cross section for polarized Z then reads

$$\frac{d\sigma_\lambda^{(0)}}{d\cos\theta} = \frac{\pi\alpha^2\beta}{16c_W^2s_W^2} \frac{M_Z^2}{(s - M_Z^2)^2} \times \begin{cases} (1 \pm \cos\theta)^2 g_e^{-2} + (1 \mp \cos\theta)^2 g_e^{+2}, & \text{for } \lambda = \pm 1, \\ 2\sin^2\theta (g_e^{-2} + g_e^{+2}) \left(1 + \frac{\beta^2 s}{4M_Z^2}\right), & \text{for } \lambda = 0, \end{cases} \quad (2)$$

with θ being the angle between \mathbf{p}_Z and \mathbf{k}_1 in the CM frame, $\beta = \frac{2|\mathbf{p}_Z|}{\sqrt{s}}$. Upon angular integration, the LO integrated cross section for polarized Z reads:

$$\sigma_\lambda^{(0)} = \frac{\pi\alpha^2\beta (g_e^{-2} + g_e^{+2})}{6c_W^2s_W^2} \frac{M_Z^2}{(s - M_Z^2)^2} \left(1 + \delta_{\lambda,0} \frac{\beta^2 s}{4M_Z^2}\right). \quad (3)$$

The total unpolarized cross section $\sigma^{(0)\text{unpol}} = \sigma_L^{(0)} + \sigma_T^{(0)} \equiv \sigma_0^{(0)} + 2\sigma_{\pm 1}^{(0)}$. In the high energy limit, the cross section for producing longitudinally-polarized Z ($\propto 1/s$) dominates the one associated with the transversely-polarized Z ($\propto 1/s^2$),

The outline of calculation for radiative corrections. As far as the $\mathcal{O}(\alpha) + \mathcal{O}(\alpha\alpha_s)$ corrections are concerned, the higher-order diagrams can be grouped into several distinct topologies as shown in Fig. 1 and Fig. 2.

It is conventional to separate the $\mathcal{O}(\alpha)$ corrections into the electromagnetic and weak corrections in a gauge-invariant manner. The NLO QED corrections as shown in Fig. 1 are usually encoded in the so-called Initial State Radiation (ISR) effect, which has been well-understood and implemented in Monte Carlo event generators. A recent study using the package WHIZARD [21] reveals that, including the ISR effect reduces the Born order $\sigma(HZ)$ at $\sqrt{s} = 250$ GeV by 10% [22]. A more careful analysis of the ISR effect for this process will be presented elsewhere.

The $\mathcal{O}(\alpha)$ and $\mathcal{O}(\alpha\alpha_s)$ corrections to the amplitude can be decomposed as follows:

$$\delta\mathcal{M}^{\sigma, \lambda} = \delta\mathcal{M}_{eeH}^{\sigma, \lambda} + \delta\mathcal{M}_{\text{Box}}^{\sigma, \lambda} + \delta\mathcal{M}_{eeZ}^{\sigma, \lambda} + \delta\mathcal{M}_{\text{S.E.}}^{\sigma, \lambda} + \delta\mathcal{M}_{ZZH}^{\sigma, \lambda} + \delta\mathcal{M}_{\gamma ZH}^{\sigma, \lambda}, \quad (4)$$

as can be recognized from Fig. 1. The first two terms corresponding to the eeH vertex corrections and box diagrams are UV-finite at $\mathcal{O}(\alpha)$.

The amplitude arising from the eeZ vertex corrections can be written as $\delta\mathcal{M}_{eeZ}^{\sigma, \lambda} = \mathcal{M}_0^{\sigma, \lambda} \hat{\Gamma}_{eeZ}^\sigma$, where the one-loop expression of the renormalized vertex form factor $\hat{\Gamma}_{eeZ}^\sigma$ is given in [19]. The amplitude also receives corrections from both ZZ and mixed γZ self-energies:

$$\delta\mathcal{M}_{\text{S.E.}}^{\sigma, \lambda} = -\mathcal{M}_0^{\sigma, \lambda} \left(\frac{\hat{\Sigma}_T^{ZZ}(s)}{s - M_Z^2} + \frac{1}{g_e^\sigma} \frac{\hat{\Sigma}_T^{\gamma Z}(s)}{s} \right), \quad (5)$$

where $\hat{\Sigma}_T$ implies the renormalized transverse part of the gauge boson self-energy.

The amplitudes involving the VZH ($V = \gamma, Z$) vertex corrections are

$$\delta\mathcal{M}_{ZZH}^{\sigma,\lambda} = \frac{e^2 g_e^\sigma M_Z}{s_W c_W} \bar{v}(k_1) \gamma_\mu P_\sigma u(k_2) \frac{1}{s - M_Z^2} \hat{\mathcal{T}}_{ZZH}^{\mu\nu} \varepsilon_{\lambda,\nu}^* \quad (6a)$$

$$\delta\mathcal{M}_{\gamma ZH}^{\sigma,\lambda} = \frac{e^2 M_Z}{s_W c_W} \bar{v}(k_1) \gamma_\mu P_\sigma u(k_2) \frac{1}{s} \hat{\mathcal{T}}_{\gamma ZH}^{\mu\nu} \varepsilon_{\lambda,\nu}^* \quad (6b)$$

By Lorentz covariance, the vertex tensor $\hat{\mathcal{T}}_{VZH}^{\mu\nu}$ can be decomposed as

$$\begin{aligned} \hat{\mathcal{T}}_{VZH}^{\mu\nu} = & T_1 k^\mu k^\nu + T_2 p_Z^\mu p_Z^\nu + T_3 k^\mu p_Z^\nu + T_4 p_Z^\mu k^\nu \\ & + T_5 g^{\mu\nu} + T_6 \epsilon^{\mu\nu\rho\sigma} k_\rho p_{Z\sigma}, \end{aligned} \quad (7)$$

where $k^\mu = p_Z^\mu + p_H^\mu$, and T_i ($i = 1, \dots, 6$) are Lorentz scalars solely depending on s , M_H^2 and M_Z^2 . Among all form factors, only T_5 is subject to renormalization, and the $\mathcal{O}(\alpha)$ counterterms for the VZH ($V = Z, \gamma$) coupling can be found in [23]. Beyond LO, the form factors T_i ($i = 1, \dots, 5$) do not vanish in general. Nevertheless, due to Furry theorem, $T_6 = 0$ for both ZZH and γZH vertex corrections through $\mathcal{O}(\alpha\alpha_s)$. Owing to the current conservation for massless electron, only $T_{4,5}$ contribute to the differential cross sections.

Some care should be exercised on the charge renormalization constant Z_e . In the so-called $\alpha(0)$ scheme, where the α is assuming its Thomson-limit value, δZ_e can be expressed as $\delta Z_e|_{\alpha(0)} = \frac{1}{2} \Pi^{\gamma\gamma}(0) - \frac{s_W}{c_W} \frac{\Sigma_T^{\gamma Z}(0)}{M_Z^2}$, where $\Pi(s) \equiv \frac{\Sigma_T^{\gamma\gamma}(s)}{s}$. The first term in $\delta Z_e|_{\alpha(0)}$ is sensitive to the hadronic contribution, thereby an intrinsic non-perturbative quantity. The hadronic contributions are often absorbed into a non-perturbative parameter, $\Delta\alpha_{\text{had}}^{(5)}(M_Z)$, which can be extracted from the measured R values in low-energy e^+e^- experiments [24]. Equivalently, one can rewrite δZ_e in $\alpha(0)$ scheme as

$$\begin{aligned} \delta Z_e|_{\alpha(0)} = & \frac{1}{2} \Delta\alpha_{\text{had}}^{(5)}(M_Z) + \frac{1}{2} \text{Re} \Pi^{\gamma\gamma(5)}(M_Z^2) \\ & + \frac{1}{2} \Pi_{\text{rem}}^{\gamma\gamma}(0) - \frac{s_W}{c_W} \frac{\Sigma_T^{\gamma Z}(0)}{M_Z^2}, \end{aligned} \quad (8)$$

where $\Pi^{\gamma\gamma(5)}(M_Z^2)$ is the photon vacuum polarization from five massless quarks at momentum transfer M_Z^2 , and $\Pi_{\text{rem}}^{\gamma\gamma}(0)$ represents the vacuum polarization from W boson, charged leptons and top quark at zero momentum transfer. Note these terms can be computed order by order in perturbation theory. Throughout this work, we only retain the top quark mass and treat the remaining five quarks massless (The effect of finite m_b will be mentioned afterwards).

Two other popular parameterization schemes are the so-called $\alpha(M_Z)$ and G_μ schemes. The corresponding charge renormalization constant can be converted from the $\alpha(0)$ scheme by $\delta Z_e|_{\alpha(M_Z)} = \delta Z_e|_{\alpha(0)} -$

$\frac{1}{2} \Delta\alpha(M_Z)$ and $\delta Z_e|_{G_\mu} = \delta Z_e|_{\alpha(0)} - \frac{1}{2} \Delta r$ respectively, where $\Delta\alpha(M_Z) = \Pi_{f \neq t}^{\gamma\gamma}(0) - \text{Re} \Pi_{f \neq t}^{\gamma\gamma}(M_Z^2)$, and the expression for the oblique parameter Δr can be found in [23]. The fine-structure constant can in turn be replaced with

$$\alpha(M_Z) = \frac{\alpha(0)}{1 - \Delta\alpha(M_Z)}, \quad (9a)$$

$$\alpha_{G_\mu} = \frac{\sqrt{2}}{\pi} G_\mu M_W^2 \left(1 - \frac{M_W^2}{M_Z^2} \right) \quad (9b)$$

in the $\alpha(M_Z)$ and G_μ schemes, respectively. In contrast to the $\alpha(0)$ scheme, these two schemes effectively resum some universal large (non-)logarithms arising from the light fermions and top quark.

The $\mathcal{O}(\alpha\alpha_s^n)$ corrections to the differential cross section read

$$\frac{d\sigma_\lambda^{(\alpha\alpha_s^n)}}{d\cos\theta} = \frac{1}{4} \frac{\beta}{32\pi s} \sum_\sigma 2\text{Re} \left[(\mathcal{M}_0^{\sigma,\lambda})^* \delta\mathcal{M}_{(\alpha\alpha_s^n)}^{\sigma,\lambda} \right] \quad (10)$$

where $n = 0, 1$ represent the $\mathcal{O}(\alpha)$ and $\mathcal{O}(\alpha\alpha_s)$ corrections, respectively.

For the actual calculation, we work in Feynman gauge and adopt the dimensional regularization to regularize the UV divergences. The Feynman diagrams and corresponding amplitudes are generated by **FeynArts** [25]. The packages **FeynCalc/FormLink** [26, 27] are employed to carry out the trace over Dirac and color matrices, and the packages **Apart** [28] and **FIRE** [29] are utilized to perform partial fraction together with integration-by-parts (IBP) reduction. We then combine **FIESTA/CubPack** [30, 31] to perform sector decomposition and subsequent numerical integrations for Master Integrals (MI) with quadruple precision.

Next-to-leading order results. First we revisit the NLO weak corrections for the Higgsstrahlung process, in line with (4) and (10). We have worked out the bare NLO amplitude analytically and also employed **LoopTools** [32] for an independent cross-check. After implementing various one-loop counterterms analytically recorded in [23], we have compared our UV-finite NLO predictions with numerous differential and integrated cross sections enumerated in [19], and found gross agreement. We have also compared our integrated NLO cross sections with those high-precision predictions tabulated in [33], which utilized the automatic package **GRACE-loop**. Reassuringly, for a variety of input values of \sqrt{s} and M_H , we always found better-than-per-mille agreement.

Mixed electroweak-QCD two-loop corrections. At $\mathcal{O}(\alpha\alpha_s)$, a simplifying pattern arises, *i.e.*, the box diagrams and eeH vertex are immune to gluonic dressing, and only those two-loop diagrams of s -channel topology in Fig. 1 survive. Concretely, the mixed electroweak-QCD 2-loop corrections to the amplitude are expressed as the last four terms in (4):

As shown in Fig. 2, QCD renormalization is fulfilled by merely inserting the top quark mass counterterm, δm_t , into the internal top quark propagator, as well as into the $Ht\bar{t}$ vertex. We take δm_t from [34]:

$$\delta m_t = -m_t \Gamma(1 + \epsilon) \left(\frac{4\pi\mu^2}{m_t^2} \right)^\epsilon \frac{C_F}{4} \frac{\alpha_s}{\pi} \frac{3 - 2\epsilon}{\epsilon(1 - 2\epsilon)}, \quad (11)$$

with the spacetime dimensions $d = 4 - 2\epsilon$.

For the $\delta\mathcal{M}_{S.E.}^{\sigma, \lambda(\alpha\alpha_s)}$ in (5), one can transplant the analytic $\mathcal{O}(\alpha\alpha_s)$ expressions of the gauge boson/Higgs self-energies from [34–36], and deduce the $\mathcal{O}(\alpha\alpha_s)$ corrections to the renormalization constants δZ_e , $\delta Z_{\gamma Z}$, $\delta Z_{Z\gamma}$, δZ_{ZZ} , δZ_H , δM_Z^2 , and δM_W^2 . Despite the absence of the $\mathcal{O}(\alpha\alpha_s)$ corrections to the bare eeZ vertex, one must incorporate the contribution to $\hat{\Gamma}_{eeZ}^{\sigma(\alpha\alpha_s)}$ that stems from the $\mathcal{O}(\alpha\alpha_s)$ counterterms, $\delta_{eeZ}^{CT\pm(\alpha\alpha_s)}$, which are UV-finite. Their numerical values in the $\alpha(0)$ scheme are

$$\delta_{eeZ}^{CT+(\alpha\alpha_s)} = \frac{\alpha\alpha_s}{\pi^2} \times (-27.33), \quad (12a)$$

$$\delta_{eeZ}^{CT-(\alpha\alpha_s)} = \frac{\alpha\alpha_s}{\pi^2} \times (+54.53). \quad (12b)$$

The values enumerated in (12) can be converted into the G_μ -scheme by subtracting $\frac{1}{2}\Delta r^{(\alpha\alpha_s)} = \frac{\alpha\alpha_s}{\pi^2} \times (+22.49)$, which then agree with [37] when adjusting the input parameters accordingly.

The real challenge is to compute the mixed electroweak-QCD corrections to VZH vertex in (6). After IBP reduction, we end up with 47 MIs associated with the bare two-loop diagrams, most of which involve four distinct scales. Fortunately, at $\sqrt{s} \sim 250$ GeV, with the aid of **CubPack** [31], we can readily obtain very accurate results for all scalar form factors T_i ($i = 1, \dots, 5$) in (7).

Ward identity for the γZH vertex demands $sT_1 + k \cdot p_Z T_4 + T_5 = 0$. We have numerically verified this relation to an extraordinary precision at $\mathcal{O}(\alpha\alpha_s)$.

Piecing together all the $\mathcal{O}(\alpha\alpha_s)$ ingredients, we obtain the differential (un)polarized cross section following (10). It is convenient to split the integrated (un)polarized cross sections into

$$\sigma_\lambda^{(\alpha\alpha_s)} = \sigma_{\lambda, Z}^{(\alpha\alpha_s)} + \sigma_{\lambda, \gamma}^{(\alpha\alpha_s)}. \quad (13)$$

For simplicity, we have combined the corrections originating from the eeZ vertex, ZZ self-energy and from the ZZH vertex together, dubbed $\sigma_{\lambda, Z}^{(\alpha\alpha_s)}$. Similarly, $\sigma_{\lambda, \gamma}^{(\alpha\alpha_s)}$ is constructed by merging the corrections from the γZ self-energy and from the γZH vertex.

Phenomenology. We will take $\sqrt{s} = 240, 250$ GeV as two benchmark energy points at Higgs factory. We adopt the following values for the input parameters [24]: $M_H = 125.09$ GeV, $M_Z = 91.1876$ GeV, $M_W = 80.385$ GeV, $m_t = 174.2$ GeV, $m_e = 0.5109989$ MeV, $m_\mu = 105.65837$ MeV, $m_\tau = 1.77686$ GeV, $G_\mu = 1.1663787 \times 10^{-5}$ GeV $^{-2}$, $\alpha(0) = 1/137.035999$, $\Delta\alpha_{\text{had}}^{(5)}(M_Z) =$

0.02764 and $\alpha(M_Z) = 1/128.943$ in the $\alpha(M_Z)$ scheme. We take $\alpha_s(M_Z) = 0.1185$ as the initial value of the QCD running coupling and $\alpha_s(\mu)$ is evaluated with package **RunDec** [38].

Table I lists our LO, NLO, and NNLO predictions to the integrated (un)polarized Higgsstrahlung cross sections in the $\alpha(0)$ scheme. While the unpolarized cross sections at $\sqrt{s} = 240, 250$ GeV are quite close in magnitude, $\sigma_L(\sigma_T)$ are slightly bigger(smaller) in the case of the higher energy. The NLO weak corrections increase the $\sigma^{(0)}$ by 3.0%(2.7%) at $\sqrt{s} = 240(250)$ GeV. The NNLO electroweak-QCD corrections turn out to be sizable, about 1.1% of the LO cross section for both CM energies.

One interesting feature can be recognized from Table I, the $\sigma_{\lambda, \gamma}^{(\alpha\alpha_s)}$ in (13) turns out to be much suppressed. This is compatible with the tiny $\mathcal{O}(\alpha\alpha_s)$ corrections to $H \rightarrow Z\gamma$ found in [39–41].

In Table II we provide our LO, NLO, NNLO predictions for the unpolarized Higgsstrahlung cross sections in the three input schemes together with the parametric uncertainty (first entry) and the QCD renormalization scale uncertainty (second entry). To assess the parametric uncertainty, we vary the values of M_W and m_t , $\Delta\alpha_{\text{had}}^{(5)}(M_Z)$ within the PDG-quoted $1 - \sigma$ error bands. For the QCD scale uncertainty, we vary the the renormalization scale μ in α_s from M_Z to \sqrt{s} .

While the parametric and scale uncertainties of the NNLO predictions in the $\alpha(0)$ and $\alpha(M_Z)$ schemes are at the level of 0.3% and 0.4% of the NNLO result, respectively, they are considerably reduced in the G_μ scheme ($\approx 0.04\%$). We also find that in the G_μ scheme the NNLO electroweak-QCD corrections only amount to 0.3% of $\sigma^{(0)}$, which is due to the fact in addition to the running of α , universal corrections to the ρ parameter are also absorbed into the LO cross section. As can also be seen in Table II, the sensitivity to the choice of input scheme is reduced at NNLO compared to NLO. To further reduce the input scheme dependence, one may have to include the two-loop electroweak corrections as well.

In Fig. 3 we show the angular distribution of (un)polarized Z boson in HZ production at a Higgs factory CM energy of 240 GeV at various levels of accuracy.

In our calculation, we neglected all quark masses except the top quark mass, and thus the b quark does not contribute to the VHZ vertex diagram. To access the validity of this approximation, we re-did our NLO and NNLO calculations by retaining $m_b = 4.66$ GeV. Due to the occurrence of the hierarchy $m_b \ll \sqrt{s} \sim M_H \sim M_Z$, this turns out to be a rather challenging calculation. We find that, keeping finite m_b reduces the NLO cross section at $\sqrt{s} = 250$ GeV by 0.05 fb, and reduces the final NNLO prediction by roughly 0.01 fb in the $\alpha(0)$ scheme. This small impact of a finite bottom quark mass is completely overwhelmed by the uncertainties listed in Table II.

\sqrt{s} (GeV)		LO (fb)	NLO Weak (fb)		NNLO mixed electroweak-QCD (fb)			
		$\sigma^{(0)}$	$\sigma^{(\alpha)}$	$\sigma^{(0)} + \sigma^{(\alpha)}$	$\sigma_Z^{(\alpha\alpha_s)}$	$\sigma_\gamma^{(\alpha\alpha_s)}$	$\sigma^{(\alpha\alpha_s)}$	$\sigma^{(0)} + \sigma^{(\alpha)} + \sigma^{(\alpha\alpha_s)}$
240	Total	223.14	6.64	229.78	2.42	0.008	2.43	232.21
	L	88.67	3.18	91.86	0.96	0.003	0.97	92.82
	T	134.46	3.46	137.92	1.46	0.005	1.46	139.39
250	Total	223.12	6.08	229.20	2.42	0.009	2.42	231.63
	L	94.30	3.31	97.61	1.02	0.004	1.02	98.64
	T	128.82	2.77	131.59	1.40	0.005	1.40	132.99

TABLE I: The (un)polarized Higgsstrahlung cross sections at $\sqrt{s} = 240$ GeV and 250 GeV in the $\alpha(0)$ scheme. Provided are the LO, NLO weak and NNLO $\mathcal{O}(\alpha\alpha_s)$ predictions as well as individual contributions for the $\mathcal{O}(\alpha)$ corrections $\sigma^{(\alpha)}$, and for the $\mathcal{O}(\alpha\alpha_s)$ corrections in (13).

\sqrt{s}	schemes	σ_{LO} (fb)	σ_{NLO} (fb)	σ_{NNLO} (fb)
240	$\alpha(0)$	223.14 ± 0.47	229.78 ± 0.77	$232.21^{+0.75+0.10}_{-0.75-0.21}$
	$\alpha(M_Z)$	252.03 ± 0.60	$228.36^{+0.82}_{-0.81}$	$231.28^{+0.80+0.12}_{-0.79-0.25}$
	G_μ	239.64 ± 0.06	$232.46^{+0.07}_{-0.07}$	$233.29^{+0.07+0.03}_{-0.06-0.07}$
250	$\alpha(0)$	223.12 ± 0.47	229.20 ± 0.77	$231.63^{+0.75+0.12}_{-0.75-0.21}$
	$\alpha(M_Z)$	252.01 ± 0.60	$227.67^{+0.82}_{-0.81}$	$230.58^{+0.80+0.14}_{-0.79-0.25}$
	G_μ	239.62 ± 0.06	231.82 ± 0.07	$232.65^{+0.07+0.04}_{-0.07-0.07}$

TABLE II: The unpolarized Higgsstrahlung cross sections at $\sqrt{s} = 240(250)$ GeV in three different input schemes. To estimate the uncertainties caused by the input parameters (first entry), we take $M_W = 80.385 \pm 0.015$ GeV, $m_t = 174.2 \pm 1.4$ GeV and $\Delta\alpha_{\text{had}}^{(5)}(M_Z) = 0.02764 \pm 0.00013$. We also change the strong coupling constant from $\alpha_s(M_Z)$ to $\alpha_s(\sqrt{s})$ (second entry) with its central value taken as $\alpha_s = \alpha_s(\sqrt{s}/2)$. For the conversion from the $\alpha(0)$ scheme to the $\alpha(M_Z)$ and G_μ schemes, we use $\Delta\alpha(M_Z)|_{\text{NLO}} = \Delta\alpha(M_Z)|_{\text{NNLO}} = 0.059$ and $\Delta r|_{\text{NLO}} = 0.0293$, $\Delta r|_{\text{NNLO}} = 0.0331$, respectively.

Summary and Outlook. Stimulated by the anticipated exquisite accuracy of the $\sigma(HZ)$ measurements in the next-generation e^+e^- Higgs factory, for the first time we calculated the mixed electroweak-QCD $\mathcal{O}(\alpha\alpha_s)$ corrections for the Higgsstrahlung process. It is found that this mixed electroweak-QCD corrections are quite sizable, about 1.1% of the LO result in $\alpha(0)$ and $\alpha(M_Z)$ schemes, well above the projected experimental (sub-)percent accuracy for the $\sigma(ZH)$ measurement. In the G_μ scheme, we find that the NNLO electroweak-QCD corrections amount to 0.3% of the LO result. A comprehensive study of parametric and QCD scale uncertainties exhibits large uncertainties in the NNLO electroweak-QCD predictions in the $\alpha(0)$ and $\alpha(M_Z)$ schemes, which however are considerably reduced in the G_μ scheme. It is important to note that to make closer contact with the actual experimental measurement, it is also useful to conduct a careful analysis on the ISR effects, as well as to study the process $e^+e^- \rightarrow \mu^+\mu^- + H$ by including the effect of finite Z width.

Note added. After this work was submitted, there also appeared an independent computation on mixed electroweak-QCD corrections to Higgsstrahlung pro-

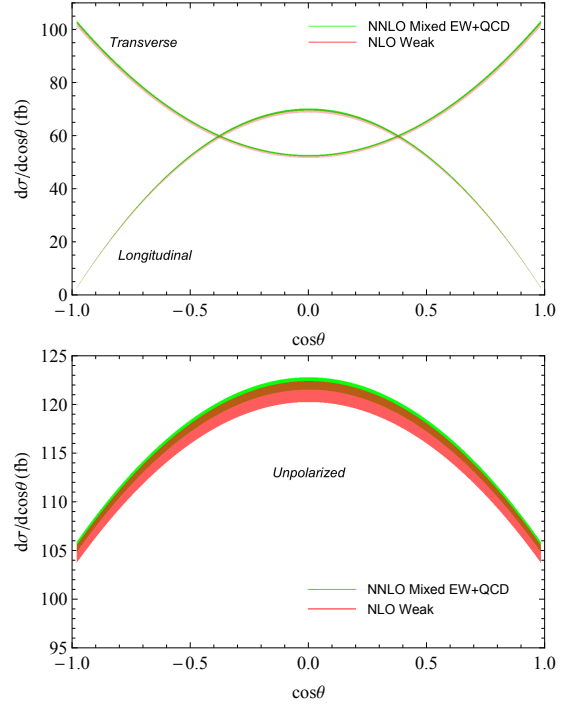


FIG. 3: Differential unpolarized/polarized cross sections for Higgsstrahlung at $\sqrt{s} = 240$ GeV at NLO $\mathcal{O}(\alpha)$ and NNLO $\mathcal{O}(\alpha\alpha_s)$. The green band indicates the uncertainties from the input parameters as adopted in Table II and the three different input schemes.

cess [42].

Acknowledgment. We are grateful to Gang Li, Xiaohui Liu and Jian-Hui Zhang for useful discussions. Q.-F. S. wishes to thank Theory Division of IHEP for warm hospitality, where this work was being finalized. Q.-F. S. is supported by the National Natural Science Foundation of China under Grant No. 11375168 and No. 11475188. The work of F. F. is supported by the National Natural Science Foundation of China under Grant No. 11505285, and by the Fundamental Research Funds for the Central Universities. The work of Y. J. is supported in part by the National Natural Science Foundation of China under Grants No. 11475188, No. 11261130311, No. 11621131001 (CRC110 by DGF and NSFC), by the IHEP Innova-

tion Grant under contract number Y4545170Y2, and by the State Key Lab for Electronics and Particle Detectors. W.-L. S. is supported by the National Natural Science Foundation of China under Grant No. 11447031 and No. 11605144, by the Natural Science Foundation of ChongQing under Grant No. cstc2014jcyjA00029, and also by the Fundamental Research Funds for the Central Universities under Grant No. XDJK2016C067. The Feynman diagrams in this paper were prepared using JaxoDraw [43, 44].

[1] G. Aad *et al.* [ATLAS Collaboration], Phys. Lett. B **716**, 1 (2012) doi:10.1016/j.physletb.2012.08.020 [arXiv:1207.7214 [hep-ex]].

[2] S. Chatrchyan *et al.* [CMS Collaboration], Phys. Lett. B **716**, 30 (2012) doi:10.1016/j.physletb.2012.08.021 [arXiv:1207.7235 [hep-ex]].

[3] H. Baer *et al.*, arXiv:1306.6352 [hep-ph].

[4] D. M. Asner *et al.*, arXiv:1310.0763 [hep-ph].

[5] M. Bicer *et al.* [TLEP Design Study Working Group], JHEP **1401**, 164 (2014) doi:10.1007/JHEP01(2014)164 [arXiv:1308.6176 [hep-ex]].

[6] CEPC-SPPC Study Group, IHEP-CEPC-DR-2015-01, IHEP-TH-2015-01, IHEP-EP-2015-01.

[7] CEPC-SPPC Study Group, IHEP-CEPC-DR-2015-01, IHEP-AC-2015-01.

[8] A. Katz and M. Perelstein, JHEP **1407**, 108 (2014) doi:10.1007/JHEP07(2014)108 [arXiv:1401.1827 [hep-ph]].

[9] C. Englert, A. Freitas, M. M. Mhlleitner, T. Plehn, M. Rauch, M. Spira and K. Walz, J. Phys. G **41**, 113001 (2014) doi:10.1088/0954-3899/41/11/113001 [arXiv:1403.7191 [hep-ph]].

[10] N. Craig, M. Farina, M. McCullough and M. Perelstein, JHEP **1503**, 146 (2015) doi:10.1007/JHEP03(2015)146 [arXiv:1411.0676 [hep-ph]].

[11] F. P. Huang, P. H. Gu, P. F. Yin, Z. H. Yu and X. Zhang, Phys. Rev. D **93**, no. 10, 103515 (2016) doi:10.1103/PhysRevD.93.103515 [arXiv:1511.03969 [hep-ph]].

[12] N. Craig, J. Gu, Z. Liu and K. Wang, JHEP **1603**, 050 (2016) doi:10.1007/JHEP03(2016)050 [arXiv:1512.06877 [hep-ph]].

[13] S. F. Ge, H. J. He and R. Q. Xiao, JHEP **1610**, 007 (2016) doi:10.1007/JHEP10(2016)007 [arXiv:1603.03385 [hep-ph]].

[14] J. R. Ellis, M. K. Gaillard and D. V. Nanopoulos, Nucl. Phys. B **106**, 292 (1976). doi:10.1016/0550-3213(76)90382-5

[15] B. L. Ioffe and V. A. Khoze, Sov. J. Part. Nucl. **9**, 50 (1978) [Fiz. Elem. Chast. Atom. Yadra **9**, 118 (1978)].

[16] J. D. Bjorken, Conf. Proc. C **7608021**, 1 (1976).

[17] J. Fleischer and F. Jegerlehner, Nucl. Phys. B **216**, 469 (1983). doi:10.1016/0550-3213(83)90296-1

[18] B. A. Kniehl, Z. Phys. C **55**, 605 (1992). doi:10.1007/BF01561297

[19] A. Denner, J. Kublbeck, R. Mertig and M. Bohm, Z. Phys. C **56**, 261 (1992). doi:10.1007/BF01555523

[20] A. Sirlin, Phys. Rev. D **22**, 971 (1980). doi:10.1103/PhysRevD.22.971

[21] W. Kilian, T. Ohl and J. Reuter, Eur. Phys. J. C **71**, 1742 (2011) doi:10.1140/epjc/s10052-011-1742-y [arXiv:0708.4233 [hep-ph]].

[22] X. Mo, G. Li, M. Q. Ruan and X. C. Lou, Chin. Phys. C **40**, no. 3, 033001 (2016) doi:10.1088/1674-1137/40/3/033001 [arXiv:1505.01008 [hep-ex]].

[23] A. Denner, Fortsch. Phys. **41**, 307 (1993) doi:10.1002/prop.2190410402 [arXiv:0709.1075 [hep-ph]].

[24] C. Patrignani *et al.* [Particle Data Group], Chin. Phys. C **40**, no. 10, 100001 (2016). doi:10.1088/1674-1137/40/10/100001

[25] T. Hahn, Comput. Phys. Commun. **140**, 418 (2001) doi:10.1016/S0010-4655(01)00290-9 [hep-ph/0012260].

[26] R. Mertig, M. Bohm and A. Denner, Comput. Phys. Commun. **64**, 345 (1991). doi:10.1016/0010-4655(91)90130-D

[27] F. Feng and R. Mertig, arXiv:1212.3522 [hep-ph].

[28] F. Feng, Comput. Phys. Commun. **183**, 2158 (2012) doi:10.1016/j.cpc.2012.03.025 [arXiv:1204.2314 [hep-ph]].

[29] A. V. Smirnov, Comput. Phys. Commun. **189**, 182 (2015) doi:10.1016/j.cpc.2014.11.024 [arXiv:1408.2372 [hep-ph]].

[30] A. V. Smirnov, Comput. Phys. Commun. **185**, 2090 (2014) doi:10.1016/j.cpc.2014.03.015 [arXiv:1312.3186 [hep-ph]].

[31] R. Cools and A. Haegemans, ACM Trans. Math. Softw. **29** (2003), no. 3 287 C296.

[32] T. Hahn and M. Perez-Victoria, Comput. Phys. Commun. **118**, 153 (1999) doi:10.1016/S0010-4655(98)00173-8 [hep-ph/9807565].

[33] G. Belanger, F. Boudjema, J. Fujimoto, T. Ishikawa, T. Kaneko, K. Kato and Y. Shimizu, Phys. Rept. **430**, 117 (2006) doi:10.1016/j.physrep.2006.02.001 [hep-ph/0308080].

[34] A. Djouadi and P. Gambino, Phys. Rev. D **49**, 3499 (1994) Erratum: [Phys. Rev. D **53**, 4111 (1996)] doi:10.1103/PhysRevD.49.3499, 10.1103/PhysRevD.53.4111 [hep-ph/9309298].

[35] A. Djouadi and P. Gambino, Phys. Rev. D **51**, 218 (1995) Erratum: [Phys. Rev. D **53**, 4111 (1996)] doi:10.1103/PhysRevD.51.218, 10.1103/PhysRevD.53.4111.2 [hep-ph/9406431].

[36] B. A. Kniehl, Phys. Rev. D **50**, 3314 (1994) doi:10.1103/PhysRevD.50.3314 [hep-ph/9405299].

[37] S. Dittmaier, A. Huss and C. Schwinn, Nucl. Phys. B **885**, 318 (2014) doi:10.1016/j.nuclphysb.2014.05.027 [arXiv:1403.3216 [hep-ph]].

[38] K. G. Chetyrkin, J. H. Kuhn and M. Steinhauser, Comput. Phys. Commun. **133**, 43 (2000) doi:10.1016/S0010-4655(00)00155-7 [hep-ph/0004189].

[39] M. Spira, A. Djouadi and P. M. Zerwas, Phys. Lett. B **276**, 350 (1992). doi:10.1016/0370-2693(92)90331-W

[40] T. Gehrmann, S. Giese and D. Kara, JHEP **1509**, 038 (2015) doi:10.1007/JHEP09(2015)038 [arXiv:1505.00561 [hep-ph]].

[41] R. Bonciani, V. Del Duca, H. Frellesvig, J. M. Henn, F. Moriello and V. A. Smirnov, JHEP **1508**, 108 (2015) doi:10.1007/JHEP08(2015)108 [arXiv:1505.00567 [hep-ph]].

[42] Y. Gong, Z. Li, X. Xu, L. L. Yang and X. Zhao, Phys. Rev. D **95**, no. 9, 093003 (2017)

doi:10.1103/PhysRevD.95.093003 [arXiv:1609.03955 [hep-ph]].

[43] D. Binosi and L. Theussl, *Comput. Phys. Commun.* **161**, 76 (2004) doi:10.1016/j.cpc.2004.05.001 [hep-ph/0309015].

[44] D. Binosi, J. Collins, C. Kaufhold and L. Theussl, *Comput. Phys. Commun.* **180**, 1709 (2009) doi:10.1016/j.cpc.2009.02.020 [arXiv:0811.4113 [hep-ph]].